ISSN 2502-5872 (Print)
ISSN 2622-3627 (Elektronik)

Volume 11 Number 2, May 2026, 373-396

OPTIMAL CONTROL MODEL FOR THE SPREAD OF RESPIRATORY INFECTIOUS DISEASES THROUGH PREVENTIVE AND TREATMENT MEASURES

Boby Rinaldi[1*], Toni Bakhtiar[2], Jaharuddin[3]

[1,2,3]Department of Mathematics, School of Data Science, Mathematics, and Informatics, IPB University, Indonesia.

*Correspondence: bobyrinaldi@apps.ipb.ac.id

ABSTRACT

Respiratory infectious diseases, including acute respiratory infections, pneumonia, MERS-CoV, and COVID-19, remain major global health concerns due to their high transmission rates and significant health and socioeconomic impacts. However, most existing models do not explicitly distinguish population groups based on behavioral factors such as mask usage nor integrate multiple interventions within a unified optimal control and cost-effectiveness framework. This study develops a modified seven-compartment epidemiological model that differentiates susceptible and infected individuals based on mask usage and incorporates four control variables: mask usage, vaccination, quarantine, and treatment. The optimal control problem is formulated using the Pontryagin Maximum Principle and solved numerically using the fourth-order Runge-Kutta method combined with the Forward-Backward Sweep Method. The results indicate that treatment is the most effective single intervention in rapidly suppressing infection, while the combination of all control measures provides the fastest overall reduction in transmission. In terms of cost-effectiveness, the four-control combination yields the lowest Average Cost-Effectiveness Ratio (ACER), indicating the highest efficiency, whereas the combination of mask usage, quarantine, and treatment produces a negative Incremental Cost-Effectiveness Ratio (ICER), implying greater health benefits at a lower additional cost compared to alternative strategies. These findings emphasize the importance of distinguishing between effectiveness and cost-efficiency in determining optimal intervention strategies.

Keywords: Optimal Control, Pontryagin Maximum Principle, Compartment Model, ICER, ACER

How to Cite: Rinaldi, B., Bakhtiar, T., & Jaharuddin, J. (2026). Optimal Control Model for The Spread of Respiratory Infectious Diseases Through Preventive and Treatment Measures. *Mathline: Jurnal Matematika dan Pendidikan Matematika, 11*(2), 373-396. http://doi.org/10.31943/mathline.v11i2.1135

PRELIMINARY

Respiratory infectious diseases, including pneumonia and coronavirus infections such as SARS, MERS, and COVID-19, remain major global health concerns due to their high transmission rates and significant mortality burden (Yin & Wunderink, 2018; World Health Organization, 2020). The global burden of these diseases continues to rise, with acute respiratory infections (ARI) accounting for nearly four million deaths annually, approximately 98% of which are caused by lower respiratory tract infections (Global Burden of Disease, 2024). Pneumonia is also recognized as the leading cause of death among children under five years old, both globally and in Indonesia, exceeding the combined deaths from AIDS, malaria, and measles (Ministry of Health of the Republic of Indonesia, 2023). This situation is further exacerbated by the emergence of novel respiratory pathogens, such as Middle East Respiratory Syndrome Coronavirus (MERS-CoV), which has demonstrated a high mortality rate since its emergence in 2012 (Yin & Wunderink, 2018).

The COVID-19 pandemic represents one of the most significant global health crises in modern history. The causative agent, Severe Acute Respiratory Syndrome Coronavirus-2 (SARS-CoV-2), is a positive single-stranded RNA virus that primarily infects the respiratory tract (Yuliana, 2020). The pandemic has demonstrated rapid transmission dynamics and substantial clinical impacts, as evidenced by epidemiological and clinical studies conducted in Wuhan, China (Chen et al., 2020; Li et al., 2020; Wang et al., 2020). Moreover, the virus exhibits high transmissibility even during early stages of infection, contributing to widespread global dissemination (He et al., 2020; Linton et al., 2020; Centers for Disease Control and Prevention, 2020). To reduce transmission, various preventive measures have been recommended, including physical distancing, mask usage, hand hygiene, mobility reduction, and avoiding crowds (World Health Organization, 2020).

Mathematical modelling has become an essential tool for understanding the dynamics of infectious disease transmission and evaluating intervention strategies. It enables the identification of key parameters influencing disease spread and provides a quantitative framework for designing effective control policies (Huppert and Katriel, 2013; da Costa et al., 2019). Numerous studies have developed mathematical models to analyze COVID-19 transmission and assess control strategies. For example, Hamdy et al. (2022) proposed a modified SEIQR model incorporating quarantine and isolation, while Mandal et al. (2020) developed an SEIR-based model to predict disease spread and evaluate intervention strategies. Furthermore, Yiran and Ning (2022) extended the SEIR model by incorporating individual protection awareness and applied the Pontryagin Maximum Principle to determine optimal control strategies alongside cost-effectiveness analysis. These studies generally indicate that combining non-pharmaceutical and pharmaceutical interventions provides effective control of disease transmission. However, most existing studies do not explicitly distinguish population groups based on behavioral factors such as mask usage within both susceptible and infected classes, nor do they comprehensively evaluate multiple intervention strategies simultaneously within an optimal control and cost-effectiveness framework.

In this study, the modeling framework of respiratory infectious disease transmission is developed using COVID-19 as a representative case, allowing the proposed model to capture realistic transmission dynamics while maintaining broader relevance to respiratory diseases. Based on this gap, this study develops a modified SEIQR model that differentiates susceptible and infected individuals based on mask usage and incorporates four control variables, namely mask usage, vaccination, quarantine, and treatment. An optimal control problem is formulated and solved using the Pontryagin Maximum Principle, while numerical solutions are obtained through the fourth-order Runge-Kutta method combined with the Forward-Backward Sweep Method. This study aims to determine the optimal implementation of these control strategies in order to identify the most effective and cost-efficient approach for reducing disease transmission in a sustainable manner.

METHODS

This study uses a mathematical modelling approach and optimal control analysis to examine the dynamics of the spread of respiratory infectious diseases and determine the most effective intervention strategies. The research steps are systematically structured to align with the characteristics of model-based research and numerical simulations. The methodological stages of this study are outlined as follows. To provide a clearer overview of the research procedure, the sequence of methodological steps is illustrated in the research flow diagram presented in Figure 1.

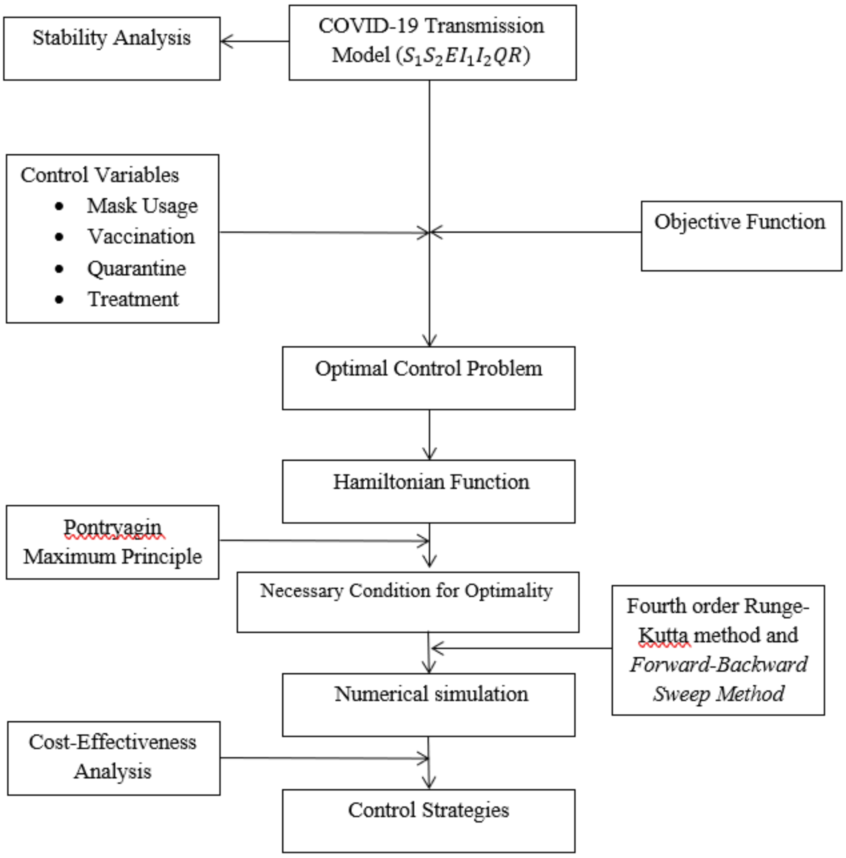

Figure 1 Research flowchart

1. Model Formulation

This section presents a mathematical model of respiratory infectious disease transmission, namely the $S_1S_2EI_1I_2QR$ model in the case of COVID-19. The population is divided into seven compartments: unmasked susceptible (S_1), masked susceptible (S_2), exposed (E), unmasked infected (I_1), masked infected (I_2), quarantined (Q), and recovered (R). The model parameters include the recruitment rate (Λ), natural death rate (μ), and disease-induced death rates (d_1, d_2, d_3) in compartments I_1, I_2, and Q. Transmission dynamics are governed by transition rates β_1, β_2, and β_3, representing movements from $S_1$to E, S_1 to S_2, and S_2 to E, respectively. The exposed compartment (E) progresses to I_1, I_2, and Q with rates δ_1, δ_2, and δ_3. Recovery occurs from $I_1$and $I_2$to $R$with rates $\sigma$and ω, respectively, while ηrepresents the transition from I_2 to Q, and ξ denotes recovery from Q to R. It is assumed that individuals in the I_2 compartment (masked infected) do not contribute to disease transmission through direct interaction, reflecting the reduced transmission risk due to consistent mask usage. The overall structure of the model is illustrated in Figure 2.

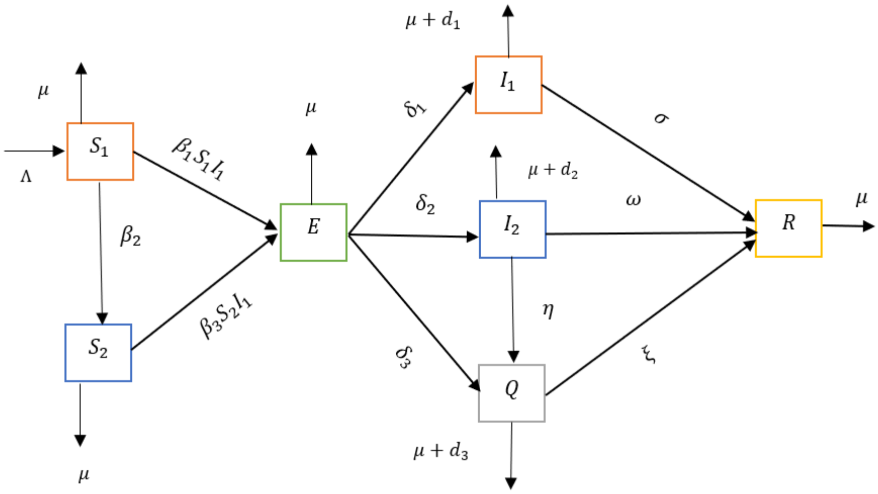

Figure 2. COVID-19 model compartment with constant control $S_1S_2EI_1I_2QR$

Figure 2 forms a non-linear ordinary differential equation which is a model of the distribution with constant control, namely:

$$
\begin{aligned}
\frac{dS_1}{dt} &= \Lambda - \mu S_1 - \beta_1 S_1 I_1 - \beta_2 S_1 \\
\frac{dS_2}{dt} &= \beta_2 S_1 - \beta_3 S_2 I_1 - \mu S_2 \\
\frac{dE}{dt} &= \beta_1 S_1 I_1 + \beta_3 S_2 I_1 - \mu E - \delta_1 E - \delta_2 E - \delta_3 E \\
\frac{dI_1}{dt} &= \delta_1 E - (\mu + d_1) I_1 - \sigma I_1 \\
\frac{dI_2}{dt} &= \delta_2 E - (\mu + d_2) I_2 - \eta I_2 - \omega I_2 \\
\frac{dQ}{dt} &= \delta_3 E + \eta I_2 - (\mu + d_3) Q - \xi Q \\
\frac{dR}{dt} &= \sigma I_1 + \omega I_2 + \xi Q - \mu R.
\end{aligned}
\tag{1}
$$

2. Model Analysis

2.1 Disease Free Equilibrium (DFE)

The disease-free equilibrium of system (1), which denotes the absence of the disease in the population or the zero value for the infectious compartments (E, I_1, I_2), is calculated by setting system equation (1) to zero and is denoted by T^0 as follows:

$$T^0 = (S_1^0, S_2^0, E^0, I_1^0, I_2^0, Q^0, R^0) = \left(\frac{\Lambda}{\beta_2 + \mu}, \frac{\beta_2 \Lambda}{\mu(\beta_2 + \mu)}, 0, 0, 0, 0, 0\right).$$

2.2 The Endemic Equilibrium Point

The endemic equilibrium of system (1) signifies the spread or outbreak of the respiratory infectious disease. The endemic equilibrium is obtained by setting system equation (1) to zero, yielding the endemic equilibrium as follows:

$$T^*(S_1, S_2, E, I_1, I_2, Q, R) = (S_1^*, S_2^*, E^*, I_1^*, I_2^*, Q^*, R^*).$$

Where,

$$S_1^* = \frac{\Lambda\beta + \Lambda d_1 + \Lambda\sigma}{\mu^2 + \mu d_1 + \mu\sigma + \mu\beta_2 + d_1\beta_2 + \sigma\beta_2 + \delta_1 E^*}$$

$$S_2^* = \frac{\beta_2\Lambda}{(\mu + \beta_2 + \beta_1 aE^*)(\beta_3 aE^* + \mu)}$$

$$E^* = \frac{\mu\beta_1 + \mu\beta_3 + \beta_2\beta_3}{2a\beta_1\beta_3} - \frac{\Lambda}{2d} + c$$

$$I_1^* = \frac{\delta_1 E^*}{d_1 + \mu + \sigma}$$

$$I_2^* = \frac{\delta_2 E^*}{d_2 + \eta + \mu + \omega}$$

$$Q^* = \frac{(\delta_3 + \eta)E^*}{d_3 + \mu + \xi}$$

$$R^* = \frac{\sigma I_1^* + \omega I_2^* + \xi Q^*}{\mu},$$

where the parameters are defined as $a = \frac{\delta_1}{\mu + d_1 + \sigma}$, $d = \mu + \delta_1 + \delta_2 + \delta_3$, and $c = \frac{\sqrt{(da\mu\beta_1 + da\mu\beta_3 + da\beta_2\beta_3 - a^2\Lambda\beta_1\beta_3)^2 - 4(da^2\beta_1\beta_3)(d\mu^2 + d\mu\beta_2 - a\Lambda\mu\beta_1)}}{2da^2\beta_1\beta_3}$.

2.3 Basic Reproduction Number

According to Brauer *et al.* (2019), the basic reproduction number ($\mathfrak{R}_0$) is an important parameter in epidemiology because it serves as a measure to determine whether an infectious disease will become an epidemic or not. The value of $\mathfrak{R}_0$ is determined using the next generation matrix method. The first step is to rewrite the system equations consisting of the exposed (E), unmasked infected (I_1), masked infected (I_2), and quarantined compartments (Q).

$$\begin{aligned}
\frac{dE}{dt} &= \beta_1 S_1 I_1 + \beta_3 S_2 I_1 - \mu E - \delta_1 E - \delta_2 E - \delta_3 E \\
\frac{dI_1}{dt} &= \delta_1 E - (\mu + d_1)I_1 - \sigma I_1 \\
\frac{dI_2}{dt} &= \delta_2 E - (\mu + d_2)I_2 - \eta I_2 - \omega I_2
\end{aligned} \tag{2}$$

$$\frac{dQ}{dt} = \delta_3 E + \eta I_2 - (\mu + d_3)Q - \xi Q.$$

From system (2), let $\mathcal{F}$ and $\mathcal{V}$ denote the vectors of new infection terms and transition terms, respectively. The matrices $F$and V, which are the Jacobian matrices of $\mathcal{F}$ and v, are obtained as follows:

$$\mathcal{F} = \begin{pmatrix} \beta_1 S_1 I_1 + \beta_3 S_2 I_1 \\ 0 \\ 0 \\ 0 \end{pmatrix}, \mathcal{V} = \begin{pmatrix} (\mu + \delta_1 + \delta_2 + \delta_3)E \\ -\delta_1 E + (\mu + d_1 + \sigma)I_1 \\ -\delta_2 E + (\mu + d_2 + \eta + \omega)I_2 \\ -\delta_3 E - \eta I_2 + (\mu + d_3 + \xi)Q \end{pmatrix}.$$

With respect to infectious compartments E, I_1, I_2 and Q, and evaluating at DFE as follows:

$$F = \begin{pmatrix} 0 & \frac{\Lambda(\beta_1+\beta_2\beta_3)}{\mu(\beta_2+\mu)} & 0 & 0 \\ 0 & 0 & 0 & 0 \\ 0 & 0 & 0 & 0 \\ 0 & 0 & 0 & 0 \end{pmatrix}, V = \begin{pmatrix} v_{11} & 0 & 0 & 0 \\ -\delta_1 & v_{22} & 0 & 0 \\ -\delta_2 & 0 & v_{33} & 0 \\ -\delta_3 & 0 & 0 & v_{44} \end{pmatrix},$$

where $v_{11} = \mu + \delta_1 + \delta_2 + \delta_3$; $v_{22} = \mu + d_1 + \sigma$; $v_{33} = \mu + d_2 + \eta + \omega$; $v_{44} = \mu + d_3 + \xi$. Represent the calculated expressions for the entries of the matrix $K = FV^{-1}$. Subsequently, following Mandal (2011), the basic reproduction number is obtained using the spectral radius of the next-generation matrix, $\Re_0 = \rho(K)$, and is derived as follows:

$$K = FV^{-1} = \begin{pmatrix} 0 & \frac{\Lambda\delta_1(\beta_1 + \beta_2\beta_3)}{v_{11}v_{22}\mu(\beta_2 + \mu)} & 0 & 0 \\ 0 & 0 & 0 & 0 \\ 0 & 0 & 0 & 0 \\ 0 & 0 & 0 & 0 \end{pmatrix}.$$

Consequently, the basic reproduction number ($\Re_0$), which is the spectral radius of the matrix K is given by:

$$\Re_0 = \frac{\delta_1\Lambda(\beta_1\mu + \beta_2\beta_3)}{\mu(\mu + \beta_2)(\delta_1 + \delta_2 + \delta_3 + \mu)(d_1 + \mu + \sigma)}.$$

2.4 Analysis of The Stability of the Disease Free Equilibrium

In this section, the criterion demonstrating the stability of the disease-free equilibrium is discussed through the proof of a stability theorem based on the basic reproduction number.

Theorem 1. The disease free equilibrium T^0 of equation (1) is locally asymptotically stable if $\Re_0 < 1$ and unstable if $\Re_0 > 1$.

Proof: The linearization process of system (1) yields the Jacobian matrix evaluated at T^0, as follows:

$$J_{T^0} = \begin{bmatrix} J_{11} & 0 & 0 & J_{14} & 0 & 0 & 0 \\ J_{21} & J_{22} & 0 & J_{24} & 0 & 0 & 0 \\ 0 & 0 & J_{33} & J_{34} & 0 & 0 & 0 \\ 0 & 0 & J_{43} & J_{44} & 0 & 0 & 0 \\ 0 & 0 & J_{53} & 0 & J_{55} & 0 & 0 \\ 0 & 0 & J_{63} & 0 & J_{65} & J_{66} & 0 \\ 0 & 0 & 0 & J_{74} & J_{75} & J_{76} & J_{77} \end{bmatrix},$$

where,

$J_{11} = -\mu - \beta_2;$ $\quad J_{14} = -\frac{\beta_1 \Lambda}{(\beta_2+\mu)};$

$J_{21} = \beta_2;$ $\quad J_{22} = -\mu;$

$J_{24} = \dfrac{-\beta_3\beta_2\Lambda}{\mu(\beta_2+\mu);}$ $\quad J_{33} = -\mu - \delta_1 - \delta_2 - \delta_3;$

$J_{34} = \dfrac{\beta_1\Lambda}{(\beta_2+\mu)} + \dfrac{-\beta_3\beta_2\Lambda}{\mu(\beta_2+\mu)};$ $\quad J_{43} = \delta_1;$

$J_{44} = -\mu - d_1 - \sigma;$ $\quad J_{53} = \delta_2;$

$J_{55} = -\mu - d_2 - \eta - \omega;$ $\quad J_{63} = \delta_3;$

$J_{65} = \eta;$ $\quad J_{66} = -\mu - d_3 - \xi;$

$J_{74} = \sigma;$ $\quad J_{75} = \omega;$

$J_{76} = \xi;$ $\quad J_{77} = -\mu.$

The eigenvalues of the Jacobian matrix evaluated at the DFE are given by

$$\lambda_{1,2} = -\mu, \lambda_3 = -(\mu+\beta_2), \lambda_4 = -(\mu + d_2 + \eta + \omega), \lambda_5 = -(\mu + d_3 + \xi).$$

Because all model parameters are positive, these five eigenvalues are strictly negative ($\lambda_i < 0,\ i = 1, \dots, 5$). The remaining two eigenvalues, λ_6 and λ_7, are obtained from the characteristic equation.

$$\lambda^2 + a_1\lambda + a_0 = 0,$$

where

$$a_1 = (\mu + d_1 + \sigma) + (\mu + \delta_1 + \delta_2 + \delta_3) > 0$$

$$a_0 = (\mu + d_1 + \sigma)(\mu + \delta_1 + \delta_2 + \delta_3) - \delta_1\left(\frac{\beta_1\Lambda}{(\beta_2+\mu)} + \frac{-\beta_3\beta_2\Lambda}{\mu(\beta_2+\mu);}\right) > 0$$

$$= (\mu + d_1 + \sigma)(\mu + \delta_1 + \delta_2 + \delta_3) - \delta_1\Lambda\left(\frac{\beta_1\mu - \beta_2\beta_3}{\mu(\beta_2+\mu)}\right) > 0$$

$$= (\mu + d_1 + \sigma)(\mu + \delta_1 + \delta_2 + \delta_3) + (1 - R_0)(\mu + d_1 + \sigma)(\mu + \delta_1 + \delta_2 + \delta_3) > 0.$$

According to the Routh–Hurwitz criterion for a second-degree polynomial, the equilibrium point is locally asymptotically stable whenever $R_0 < 1$, because both conditions $a_1 > 0$ and $a_0 > 0$ are satisfied, which ensures that λ_6 and λ_7 have negative real parts and, therefore, all eigenvalues of the Jacobian matrix are negative (Murray, 2002).

3. Optimal Control Problem

This section discusses the optimal control problem. The objective is to determine the best prevention and treatment strategies for respiratory infectious diseases by incorporating four optimal control variables: mask usage (u), vaccination (v), quarantine (q), and treatment (ψ). These control variables are introduced to enhance the effectiveness of intervention strategies compared to system (1), which is formulated under constant control parameters.

In particular, several model parameters are reformulated into time-dependent control variables to reflect dynamic intervention strategies. The parameter β_2, which represents the transition rate influenced by mask usage, is replaced by the control variable $u(t)$ to allow adaptive regulation of mask compliance over time. Similarly, the parameters δ_3 and η, which are associated with quarantine-related transitions, are replaced by the control variable $q(t)$. Furthermore, the recovery-related parameters $\sigma$and ω are replaced by the treatment control variable $\psi(t)$, enabling the modeling of time-dependent treatment efforts.

This transformation allows the model to capture more realistic and flexible intervention policies, where control measures can vary over time rather than remain constant. Thus, the model for the spread of respiratory infectious diseases with control variables is given as follows:

$$
\begin{aligned}
\frac{dS_1}{dt} &= \Lambda - \mu S - \beta_1 S_1 I_1 - v(t) S_1 - u(t) S_1 \\
\frac{dS_2}{dt} &= u(t) S_1 - \beta_3 S_2 I_1 - \mu S_2 - v(t) S_2 \\
\frac{dE}{dt} &= \beta_1 S_1 I_1 + \beta_3 S_2 I_1 - \mu E - \delta_1 E - \delta_2 E - q(t) E \\
\frac{dI_1}{dt} &= \delta_1 E - (\mu + d_1) I_1 - \psi(t) I_1 \\
\frac{dI_2}{dt} &= \delta_2 E - (\mu + d_2) I_2 - q(t) I_2 - \psi(t) I_2 \\
\frac{dQ}{dt} &= q(t) E + q(t) I_2 - (\mu + d_3) Q - \xi Q \\
\frac{dR}{dt} &= \psi(t) I_1 + \psi(t) I_2 + \xi Q + v S_1 + v S_2 - \mu R.
\end{aligned}
\tag{3}
$$

Based on equation system (3), an objective function can be formed with control variables u, v, q, ψ, which can minimize the number of infected individuals (I_1, I_2) and exposed individuals (E). The control variables u, v, q, and ψ are assumed to be bounded functions satisfying $0 \le u \le u_{\max}, 0 \le v \le v_{\max}, 0 \le q \le q_{\max}, 0 \le \psi \le \psi_{\max}$. Thus, the objective function of this optimal control can be mathematically expressed as follows:

$$\min J = \int_{t_0}^{t_f} \{A_1 I_1 + A_2 I_2 + A_3 E + \tfrac{1}{2}(B_1 u^2 + B_2 v^2 + B_3 q^2 + B_4 \psi^2)\} dt, \tag{4}$$

where A_1, A_2, A_3 are the respective weights for infected individuals without masks (I_1), infected individuals with masks (I_2), and exposed individuals (E). $B_{i,}\ i = 1, 2, 3, 4$ Meanwhile is the cost required for each control measure in disease control (Tu 1994).

3.1 Hamilton Function

Based on Pontryagin Maximum Principle, the Hamiltonian associated with the proposed optimal control problem is defined as follows:

$$\begin{aligned}
\mathcal{H} = {} & A_1 I_1 + A_2 I_2 + A_3 E + \frac{1}{2}(B_1 u^2 + B_2 v^2 + B_3 q^2 + B_4 \psi^2) \\
& + p_1(\Lambda - \mu S_1 - \beta_1 S_1 I_1 - v S_1 - u S_1) + p_2(u S_1 - \beta_3 S_2 I_1 - \mu S_2 - v S_2) \\
& + p_3(\beta_1 S_1 I_1 + \beta_3 S_2 I_1) - \mu E - \delta_1 E - \delta_2 E - q E) + p_4(\delta_1 E \\
& - (\mu + d_1) I_1 - \psi I_1 + p_5(\delta_2 E - (\mu + d_2) I_2 - q I_2 - \psi I_2) \\
& + p_6(q E + q I_2 - (\mu + d_3) Q - \xi Q) \\
& + p_7(\psi I_1 + \psi I_2 + \xi Q + v S_1 + v S_2 - \mu R),
\end{aligned}$$

where $p_i \neq 0 (i = 1, \dots, 7)$ denotes the Lagrange multipliers.

3.2 Application of Pontryagin Maximum Principle

The optimal conditions of the problem in the Hamiltonian function can be obtained by satisfying the necessary conditions for optimality in Pontryagin Maximum Principle. The The necessary conditions for optimality are obtained by differentiating the Hamiltonian function with respect to each control variable. The optimal controls are given by

$$u^*(t) = \min \left\{ u_{\max}, \max \left\{ 0, \frac{(p_1 - p_2) S_1}{B_1} \right\} \right\},$$

$$v^*(t) = \min \left\{ v_{\max}, \max \left\{ 0, \frac{(p_1 - p_7) S_1 + (p_2 - p_7) S_2}{B_2} \right\} \right\},$$

$$q^*(t) = \min \left\{ q_{\max}, \max \left\{ 0, \frac{(p_3 - p_6) E + (p_5 - p_6) I_2}{B_3} \right\} \right\},$$

$$\psi^*(t) = \min\left\{\psi_{\max}, \max\left\{0, \frac{(p_4 - p_7)I_1 + (p_5 - p_7)I_2}{B_4}\right\}\right\}.$$

Then, the optimal state system (constraint equations) is derived from the Hamiltonian. Let $x = (S_1, S_2, E, I_1, I_2, Q, R)$ denote the state variables. According to the Pontryagin Maximum Principle, the state equations are given by

$$\dot{x}_i(t) = \frac{\partial H}{\partial p_i}, i = 1, \dots, 7.$$

The resulting state system corresponds to the controlled model described in Equation (3). The next step is to determine the adjoint system solution by solving $\dot{p}(t) = -\frac{\partial \mathcal{H}}{\partial x}$ with , so that we get $x \in \{S_1, S_2, E, I_1, I_2, Q, R\}$

$$\dot{p}_1 = -\frac{\partial \mathcal{H}}{\partial S_1} = p_1(\mu + \beta_1 I_1 + v + u) - p_2 u - p_3 \beta_1 I_1 - p_7 v,$$
$$\dot{p}_2 = -\frac{\partial \mathcal{H}}{\partial S_2} = p_2(\beta_3 I_1 + \mu + v) - p_3 \beta_3 I_1 - p_7 v,$$
$$\dot{p}_3 = -\frac{\partial \mathcal{H}}{\partial E} = -A_3 + p_3(\mu + \delta_1 + \delta_2 + q) - p_4 \delta_1 - p_5 \delta_2 - p_6 q,$$
$$\dot{p}_4 = -\frac{\partial \mathcal{H}}{\partial I_1} = -A_1 + p_1 \beta_1 S_1 - p_2 \beta_3 S_2 - p_3(\beta_1 S_1 + \beta_3 S_2) + p_4(\mu + d_1 + \psi) - p_7 \psi,$$
$$\dot{p}_5 = -\frac{\partial \mathcal{H}}{\partial I_2} = -A_2 + p_5(\mu + d_2 + q + \psi) - p_6 q - p_7 \psi,$$
$$\dot{p}_6 = -\frac{\partial \mathcal{H}}{\partial Q} = p_6(\mu + d_3 + \xi) - p_7 \xi,$$
$$\dot{p}_7 = -\frac{\partial \mathcal{H}}{\partial R} = p_7 \mu.$$

Since the final time t_f is fixed and the terminal states are free, with no terminal cost included in the objective functional, the transversality conditions are given by $p_k(t_f) = 0, k = 1,2,3,4,5,6,7$.

RESULT AND DISCUSSION

The results and discussion section presents the numerical simulation output of the optimal control model and an interpretation of the dynamics that emerge in each compartment. The analysis is conducted by examining the effect of each intervention strategy, both single control strategies and combinations of controls, on suppressing disease spread. The numerical simulations are performed using the fourth-order Runge–Kutta method within the Forward-Backward Sweep framework, involving an iterative process that solves the state system forward in time and the costate system backward in time. The findings are systematically compared to identify patterns, effectiveness, as well as the mathematical and epidemiological implications of the tested control strategies.

1. Numerical Simulation

Numerical simulations were conducted to observe the dynamics of the optimal control model over a time horizon of 100 days. The weight parameters for the objective function were set as $A_1 = 150$, $A_2 = 100$, and $A_3 = 50$, while the intervention cost parameters were $B_1 = 1$, $B_2 = 10$, $B_3 = 5$, and $B_4 = 10$. These values were selected heuristically to reflect realistic relative magnitudes of health impacts and intervention costs. In particular, the cost of mask usage is assumed to be lower than vaccination, while the cost associated with untreated infected individuals (I_1) is considered higher than that of individuals with protective awareness (I_2), reflecting differences in healthcare burden and transmission risk. Based on the Pontryagin Maximum Principle, the optimal control formulation yields two coupled systems of differential equations: the state system and the adjoint system. The state system, subject to initial conditions, is solved forward in time, while the adjoint system, subject to transversality (final) conditions, is solved backward in time (Bakhtiar and Hanum, 2014).

The simulations consider a total of 15 optimal control strategies in addition to the constant control scenario. These strategies are categorized into two groups: single control strategies and multiple control strategies. Prior to conducting the numerical simulations, all parameter values used in the model are summarized in Table 1.

Table 1. Parameter value

Parameter	Value	Unit	Reference
Λ	0,000039	days^{-1}	Hethcote (2000)
μ	0,000028	days^{-1}	Assumed
d_1, d_2, d_3	0,00000357	days^{-1}	CDC (2020)
Parameter	**Value**	**Unit**	**Reference**
β_1	0,7	days^{-1}	Van den Driessche and Watmough (2002)
β_2	0,1	days^{-1}	Assumed
β_3	0,4	days^{-1}	Assumed
δ_1	0,2	days^{-1}	WHO (2020)
δ_2	0,2	days^{-1}	WHO (2020)
δ_3	0,156	days^{-1}	Linton *et al* (2020)

Parameter	Value	Unit	Reference
σ	0,14	days^{-1}	Chen *et al* (2020)
ξ	0,2	days^{-1}	He *et al* (2020)
η	0,1	days^{-1}	Li *et al* (2020)
ω	0,071	days^{-1}	Wang *et al* (2020).

Using the parameter values in Table 1, the optimal control model is numerically simulated by considering four control variables. This results in fifteen distinct control strategies, including both single-control and multiple-control implementations, as presented in Table 2.

Table 2. Optimal control implementation strategy

Control	Strategy	$\boldsymbol{u}$	$\boldsymbol{v}$	$\boldsymbol{q}$	$\boldsymbol{\psi}$
Single	1	●			
	2		●		
	3			●	
	4				●
Two	5	●	●		
	6	●		●	
	7	●			●
	8		●	●	
	9		●		●
	10			●	●
Control	**Strategy**	$\boldsymbol{u}$	$\boldsymbol{v}$	$\boldsymbol{q}$	$\boldsymbol{\psi}$
Three	11	●	●	●	
	12	●	●		●
	13	●		●	●
	14		●	●	●
Four	15	●	●	●	●

The strategy is divided into two parts, namely single control and multiple control, where single control is the application of intervention from one optimal control in the infectious compartment (E, I_1, I_2) and multiple control is a combination strategy of several controls such as a combination of 2 controls, a combination of 3 controls and a combination of 4 controls.

1.1 Single Control Strategy

The single control strategy involves applying optimal control to the infectious compartments, namely the exposed compartment (E), infected without a mask (I_1), and infected with a mask (I_2), by comparing the results with those obtained under constant control. In this context, the constant control simulation represents the baseline scenario, corresponding to the numerical simulation of the original model without the inclusion of optimal control variables. This baseline serves as a fundamental reference point for evaluating the effectiveness of each optimal control strategy in reducing disease transmission. The graphical results for the single control strategy are presented in Figure 3, Figure 4, and Figure 5.

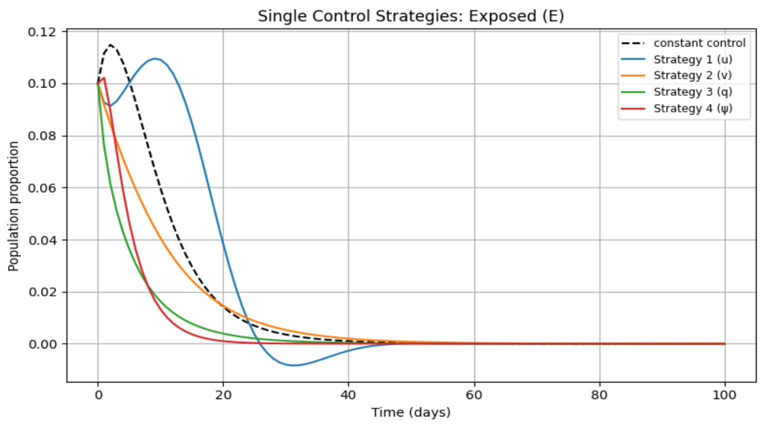

Figure 3. The effect of optimal control and constant control on compartments *E*

Figure 3 shows that the best optimal control is treatment control (ψ), followed by quarantine control (q), vaccination (v), and masks (u). Treatment control can be seen to reduce the proportion E to 0 on day 20, while quarantine takes a little longer, namely day 40, and vaccination and mask control on a similar day, namely day 45, and constant control on a day that is almost the same as vaccination and masks.

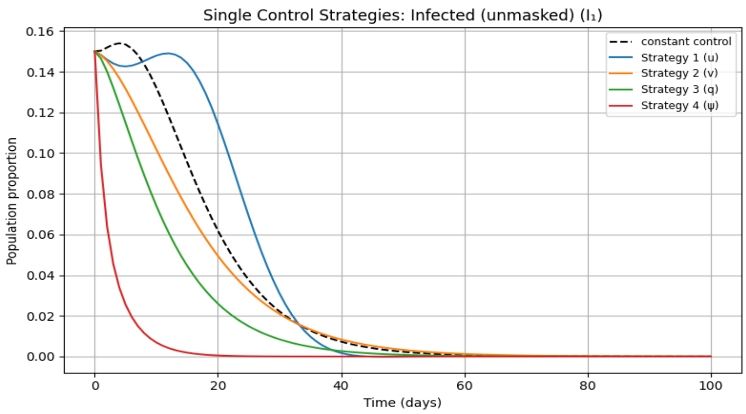

Figure 4. The effect of optimal control and constant control on compartments I_1

Figure 4 shows that the best optimal control is the treatment control (ψ) , which reduces the proportion of infections without masks (I_1) to 0 on day 18. The second-best optimal control, which rapidly reduces I_1 is the mask control (u) on day 50. Quarantine control is the third control to reduce the proportion I_1 , on day 60, and last is the vaccination control and constant control on day 65.

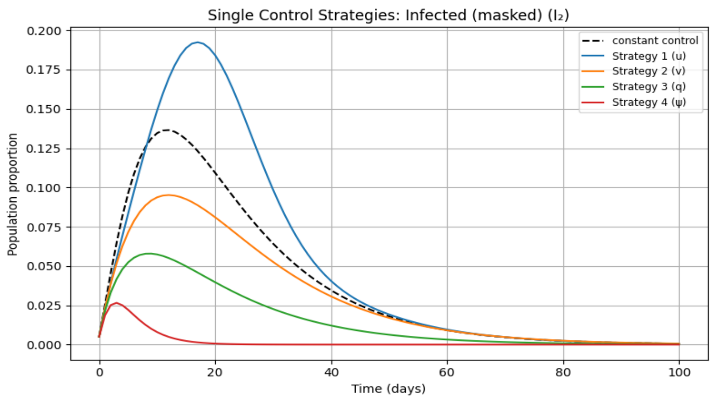

Figure 5. The effect of optimal control and constant control on compartments I_2

Figure 5 shows that the masked infection compartment (I_2) experienced a drastic decrease towards 0 due to the influence of treatment control on the 20th day. Then there was quarantine control (ψ) which suppressed the compartment I_2 towards 0 on the 50th day. Then there was mask control, vaccination and constant control which reduced the proportion on I_2 the 60th day.

In *the single control,* it can be seen that the best optimal control to suppress the infectious compartment is treatment control (ψ), followed by quarantine control (q), then masks (u), and vaccination (v).

1.2 Multiple Control Strategy

The multiple control strategy is a combination control strategy of several optimal controls consisting combinations of 2 controls, 3 controls, and 4 controls. The combination of 2 controls in a E compartment can be seen in Figure 6 below.

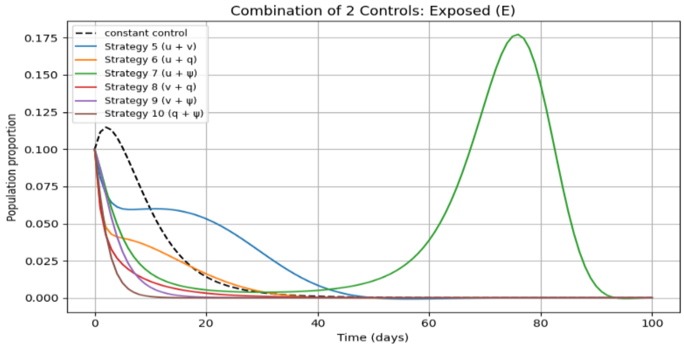

Figure 6. The effect of the combination of 2 controls on the compartment E

Figure 6 shows that there are 6 strategies from a combination of 2 controls, and it can be seen that the best strategy for reducing the number of compartments E is the control strategy of quarantine (q) and treatment with a drastic decrease to a value of 0 on day 12. Next is the control strategy that suppresses the spread rate in the compartment E, namely vaccination (v) and treatment (ψ), which takes approximately 18 days. Then there is a combination of vaccination (v) and quarantine (q). The strategy that takes the longest to suppress the compartment E is the control strategy of masks (u) and treatment, which takes 90 days due to a rebound on day 60. The effect of the 2 control strategies on the compartment I_1 can be seen in Figure 7 below.

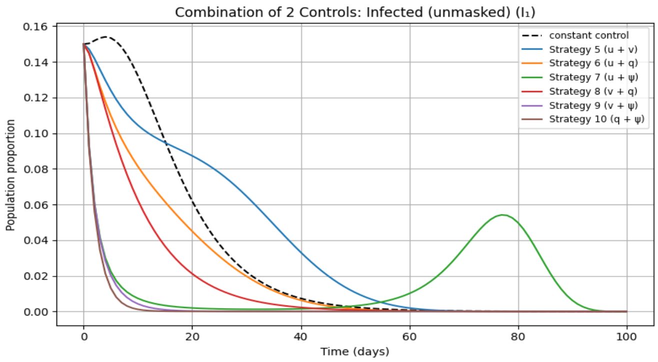

Figure 7. The effect of the combination of 2 controls on the compartment I_1

Figure 7 shows the dynamics in the compartment I_1 caused by the influence of the two optimal control combinations. It can be seen that the best two control strategy is the combination of quarantine control (q) and treatment (ψ), which requires 12 days to suppress the spread I_1. The second-best two-control strategy that suppresses the spread I_1 quickly is the combination of vaccination control (v) and treatment (ψ), which requires 15 days. The effect of the two-control strategy on the compartment I_2 can be seen in Figure 8 below.

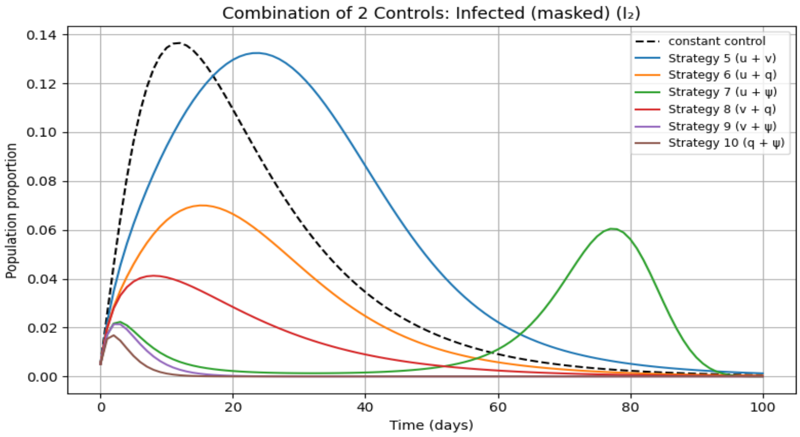

Figure 8. The effect of the combination of 2 controls on the compartment I_2

Figure 8 shows the changes that occur in the compartment I_2 caused by the combined effects of the two optimal control strategies. The figure shows that the combination that most rapidly reduces the proportion in the infectious compartment (I_2) is the combination of quarantine control (q) and treatment (ψ). The second combination that can rapidly reduce the spread (I_2) is vaccination (v) and treatment (ψ). The combination that takes the longest to reduce the proportion in the infectious compartment (I_2) is the combination of mask control (u) and vaccination (v), constant control and mask control (u), and treatment (ψ). Thus, it can be concluded that the two optimal control strategies that most quickly suppress the spread in the infectious compartment are the combination of quarantine control (q) and treatment (ψ) and the combination of vaccination(v) and treatment (ψ). Strategies combining the three optimal controls aimed at suppressing infectious compartments such as the exposed compartment (E) , unmasked infection (I_1), and masked infection (I_2) can be seen in Figures 9, 10, and 11 below.

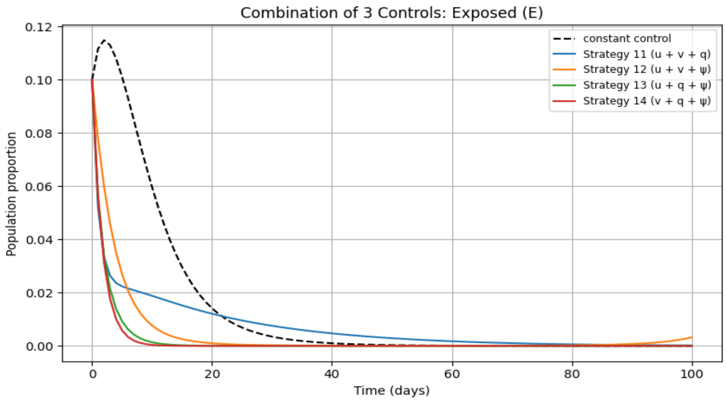

Figure 9. The effect of the combination of 3 controls on the compartment *E*

Figure 9 shows that the exposed compartment (E) decreases due to the influence of the combined 3 control strategies. The fastest strategy in suppressing the compartment E is the combination of vaccination (v), quarantine (q), and treatment (ψ) with the time required to reduce the proportion E to 10 days. Meanwhile, the longest strategy in reducing the proportion E is the combination of mask control (u), vaccination (v), and treatment (ψ) with the time required being 70 days.

The dynamics of the infection compartment without masks (I_1) influenced by the optimal control strategy with a combination of 3 controls can be seen in Figure 10 below

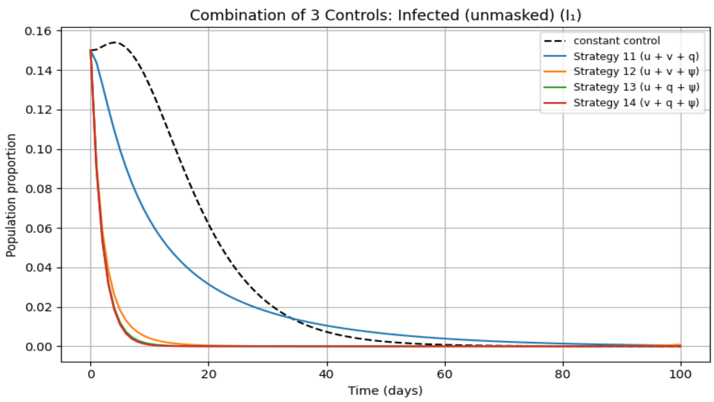

Figure 10. The effect of the combination of 3 controls on the compartment I_1

Figure 10 shows that there are two control strategies that have similar results: the combination of vaccination control (v), quarantine (q), and treatment (ψ), and the combination of mask control (u), quarantine (q), and treatment (ψ) which requires 10 days to suppress the compartment (I_1). Meanwhile, the combination of three controls that takes the longest to reduce the compartment (I_1) is the strategy combining mask control (u), vaccination (v), and quarantine (q), which requires 80 days.

The dynamics of the I_2 compartments affected by the strategy consisting of a combination of 3 controls can be seen in Figure 11 below.

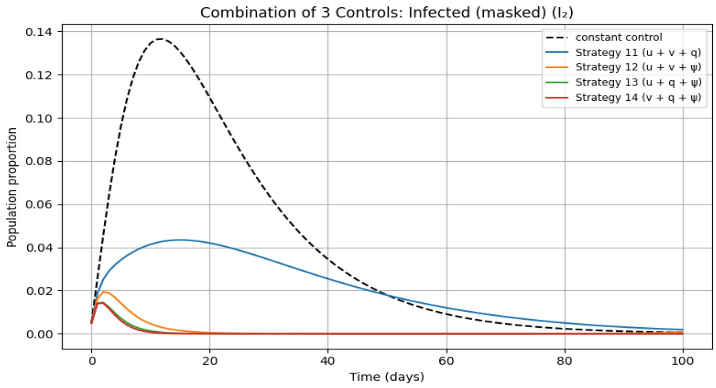

Figure 11. The effect of the combination of 3 controls on the compartment I_2

Figure 11 shows that the three best control strategies that suppress the spread rate in the masked infection compartment (I_2) are the vaccination control strategy (v), quarantine (q), and treatment (ψ), as well as strategies with similar results, namely the optimal mask control strategy (u), quarantine (q), and treatment (ψ), with a duration of 10 days required to suppress the spread. Meanwhile, the optimal control strategy that takes the longest to suppress the spread is masks (u), vaccination (v), and quarantine (q), which requires 100 days.

The strategy representing the combination of all optimal controls, referred to as Strategy 15, is illustrated in Figure 12, 13, and 14.

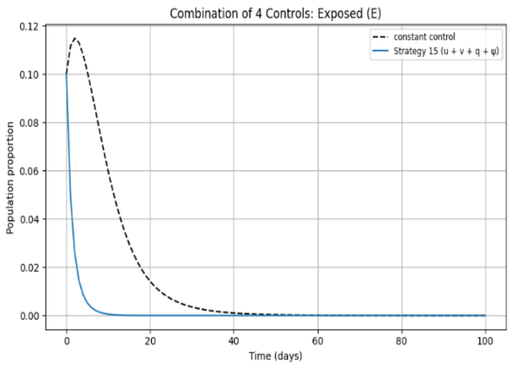

Figure 12. The effect of the combination of 4 optimal control on the compartment E

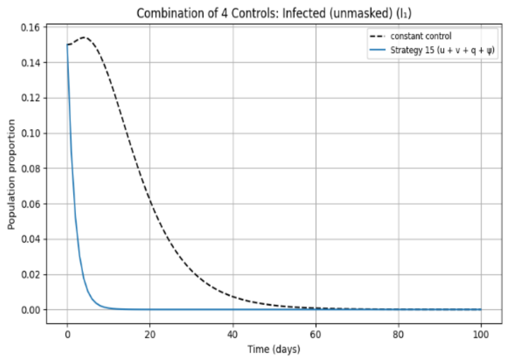

Figure 13. The effect of the combination of 4 optimal control on the compartment I_1

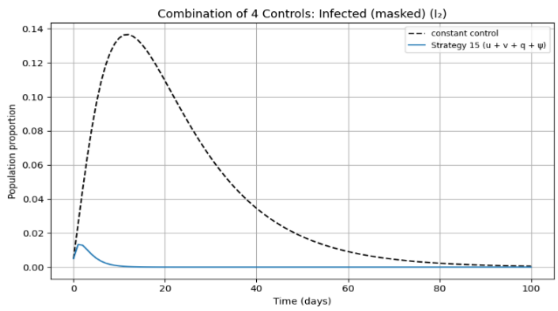

Figure 14. The effect of the combination of 4 optimal control on the compartment I_2

Figure 11, 12, and 13 shows that the combination of the four optimal controls has a very significant effect in suppressing the spread. Figures 11, 12, and 13 are visualizations of the effect of the strategy with 4 controls on the infectious compartment, with the time required being around 10 days to suppress the proportion of the compartment E, I_1, I_2.

1.3 Cost Effectiveness Analysis

Health resources can be allocated optimally to achieve maximum health benefits. ACER represents the average cost per unit of health benefit. Meanwhile, ICER determines the incremental costs incurred per unit. According to Asamoah *et al.* (2022), the ACER and ICER formulas are as follows:

$$\text{ACER} = \frac{\text{Total expenses incurred}}{\text{Total number of infections avoided}}$$

$$\text{ICER} = \frac{\text{Total cost change in p and q strategies}}{\text{Changes in control benefits in p and q strategies}}$$

The results of total costs, benefits and ACER will be stated in table 3.

Table 3. ACER value calculation result

Strategy	Total cost	Benefits	ACER
1	5.791007	1.488734	3.889888
2	178.989599	50.572114	3,539294
5	183.463519	51,592574	3.556006
15	183.993157	81.597450	2.254889
14	186.055226	81.595762	2,280207
9	216.648035	81.266583	2.665893
8	222,288650	64.521274	3.445199
11	224.426756	64.663591	3,470682
3	225.469059	56.979902	3.956993
13	241.615448	81.566670	2,962184
12	214.435653	81.276331	2.638353
6	279,163748	57.294662	4.872422

Strategy	Total cost	Benefits	ACER
7	281,130828	81.145817	3.464514
10	303,167886	81.564205	3.716923
4	360,186059	81.080755	4.442313

Based on Table 3, the most cost-efficient strategy is identified as strategy 15, which represents the combination of all control measures. This strategy yields the smallest Average Cost-Effectiveness Ratio (ACER) value of 2.254889, indicating that it provides the greatest health benefit per unit cost compared to other strategies. Therefore, the implementation of combined interventions namely mask usage, vaccination, quarantine, and treatment offers the most efficient approach in controlling the spread of the disease The incremental ratios are then evaluated between consecutive non-dominated strategies, and the resulting ICER values are presented in Table 4.

Table 4. ICER value calculation results

Strategy	COST	Benefit	ICER
Constan control	0	0	-
1	5,791007	1,488734	3.889888
2	178,989599	50,572114	3,528661
15	183,993157	81,597450	0,161274

The cost-effectiveness analysis was conducted following standard procedures by ranking strategies based on increasing effectiveness. Dominated and extendedly dominated strategies were eliminated prior to ICER calculation to ensure valid comparisons. The ICER values were then computed incrementally among the remaining non-dominated strategies, as presented in Table 4. The results indicate that Strategy 15 provides the most cost-effective outcome, as it yields the lowest ICER value, meaning it achieves the greatest additional benefit with the least additional cost compared to other strategies.

CONCLUSION

The mathematical model of respiratory infectious disease is formulated as a modified SEIQR model with seven compartments $(S_1, S_2, E, I_1, I_2, Q, R)$. An optimal control framework is incorporated, consisting of four control variables: three preventive controls mask usage (u), vaccination (v), and quarantine (q) and one treatment control (ψ). The implementation of optimal control is divided into single and multiple control strategies. In the single-control scenario, treatment (ψ) is the most effective in rapidly reducing the infectious compartment by 10% within an average of 20 days, outperforming the other controls.

For multiple control strategies, the best two-control combination is quarantine (q) and treatment (ψ), while the best three-control strategy consists of vaccination (v), quarantine (q), and treatment (ψ). The combination of all four controls is the most effective overall, achieving the fastest reduction in the infectious population. From a cost-effectiveness perspective, this four-control strategy yields the smallest Average Cost-Effectiveness Ratio (ACER) value, indicating the highest average efficiency. However, after applying standard cost-effectiveness analysis procedures by eliminating dominated and extendedly dominated strategies, the Incremental Cost-Effectiveness Ratio (ICER) results indicate that Strategy 15 is the most cost-effective option, as it provides the greatest additional health benefit with the lowest incremental cost compared to other feasible strategies. This finding highlights the importance of applying proper ICER methodology to ensure valid and reliable decision-making.

However, this study has several limitations, as the model assumes a closed population without considering population mobility or demographic changes. Therefore, future research is recommended to extend the model by incorporating more realistic population dynamics and by differentiating mask control based on COVID-19 variants, such as Delta, Omicron, and other emerging variants.

REFERENCES

Asamoah, J. K. K., Okyere, E., Abidemi, A., Moore, S. E., Sun, G. Q., Jin, Z., Acheampong, E., & Gordon, J. F. (2022). Optimal control and comprehensive cost-effectiveness analysis for COVID-19. *Results in Physics, 33*, 105177. https://doi.org/10.1016/j.rinp.2022.105177

Bakhtiar, T., & Hanum, F. (2014). Epidemic control model with vaccination and treatment. *Proceedings of the National Mathematics Seminar, 2*(1), 315–322.

Brauer, F., Castillo-Chavez, C., & Feng, Z. (2019). *Mathematical models in epidemiology*. New York, NY: Springer.

Centers for Disease Control and Prevention. (2020). *COVID-19 pandemic planning scenarios*. https://www.cdc.gov/coronavirus/2019-ncov/hcp/planning-scenarios.html

Chen, N., Zhou, M., Dong, X., Qu, J., Gong, F., Han, Y., & Zhang, L. (2020). Epidemiological and clinical characteristics of 99 cases of 2019 novel coronavirus pneumonia in Wuhan, China: A descriptive study. *The Lancet, 395*(10223), 507–513. https://doi.org/10.1016/S0140-6736(20)30211-7

Da Costa, A. L. P., Neto, O. A. R., & Silva-Júnior, A. C. S. (2019). Conditioners of the infectious disease dynamics. *Estação Científica, 8*(3), 9–23. https://doi.org/10.18468/estcien.2018v8n3.p09-23

Global Burden of Disease. (2024). Global, regional, and national incidence and mortality burden of non-COVID lower respiratory infections and aetiologies 1990–2021: A systematic analysis from the Global Burden of Disease Study 2021. *The Lancet*. https://doi.org/10.1016/S1473-3099(24)00176-2

Hamdy, M. Y., Alghamdi, S. M., El-Shafie, A., & Abbas, H. M. (2022). A proposed modified SEIQR epidemic model to analyze the COVID-19 spreading in Saudi Arabia. *Alexandria Engineering Journal, 61*, 2456–2470. https://doi.org/10.1016/j.aej.2021.06.095

He, X., Lau, E. H. Y., Wu, P., Deng, X., Wang, J., Hao, X., Lau, Y. C., Wong, J. Y., Guan, Y., Tan, X., & Mo, X. (2020). Temporal dynamics in viral shedding and transmissibility of COVID-19. *Nature Medicine, 26*(5), 672–675. https://doi.org/10.1038/s41591-020-0869-5

Heath, M. (2002). *Scientific computing: An introduction* (2nd ed.). New York, NY: McGraw-Hill.

Hethcote, H. (2000). The mathematics of infectious diseases. *SIAM Review, 42*, 599–653. https://doi.org/10.1137/S0036144500371907

Huppert, A., & Katriel, G. (2013). Mathematical modeling and prediction in infectious disease epidemiology. *Clinical Microbiology and Infection, 19*(11), 999–1005. https://doi.org/10.1111/1469-0691.12308

Kouidere, A., Kada, D., Balatif, O., Rachik, M., & Naim, M. (2021). Optimal control approach of a mathematical modeling with multiple delays of the negative impact of delays in applying preventive precautions against the spread of the COVID-19 pandemic. *Chaos, Solitons & Fractals, 142*, 110438. https://doi.org/10.1016/j.chaos.2020.110438

Li, Q., Guan, X., Wu, P., Wang, X., Zhou, L., Tong, Y., & Feng, Z. (2020). Early transmission dynamics in Wuhan, China, of novel coronavirus–infected pneumonia. *New England Journal of Medicine, 382*(13), 1199–1207. https://doi.org/10.1056/NEJMoa2001316

Linton, N. M., Kobayashi, T., Yang, Y., Hayashi, K., Akhmetzhanov, A. R., Jung, S. M., & Nishiura, H. (2020). Incubation period and other epidemiological characteristics of 2019 novel coronavirus infections. *Journal of Clinical Medicine, 9*(2), 538. https://doi.org/10.3390/jcm9020538

Mandal, M., Jana, S., Nandi, S. K., Khatua, A., Adak, S., & Kar, T. K. (2020). A model-based study on the dynamics of COVID-19: Prediction and control. *Chaos, Solitons & Fractals, 136*, 109889. https://doi.org/10.1016/j.chaos.2020.109889

Ministry of Health of the Republic of Indonesia. (2023). *The government is committed to reducing deaths due to pneumonia*. https://www.kemkes.go.id

Murray, J. D. (2002). *Mathematical biology I: An introduction* (3rd ed.). Springer.

Pontryagin, L. S., Boltyanskii, V. G., Gamkrelidze, R. V., & Mishchenko, E. F. (1962). *The mathematical theory of optimal processes*. New York, NY: CRC Press.

Tu, P. N. V. (1994). *Dynamical systems: An introduction with applications in economics and biology* (2nd ed.). Heidelberg: Springer-Verlag.

Van den Driessche, P., & Watmough, J. (2002). Reproduction numbers and sub-threshold endemic equilibria for compartmental models of disease transmission. *Mathematical Biosciences, 180*, 29–48. https://doi.org/10.1016/S0025-5564(02)00108-6

Wang, D., Hu, B., Hu, C., Zhu, F., Liu, X., Zhang, J., & Zhao, Y. (2020). Clinical characteristics of 138 hospitalized patients with 2019 novel coronavirus–infected pneumonia in Wuhan, China. *JAMA, 323*(11), 1061–1069. https://doi.org/10.1001/jama.2020.1585

World Health Organization. (2020). *Transmission of SARS-CoV-2: Implications for infection prevention precautions*. https://cdn.who.int

Yin, Y., & Wunderink, R. G. (2018). MERS, SARS and other coronaviruses as causes of pneumonia. *Respirology, 23*(2), 130–137. https://doi.org/10.1111/resp.13155

Yiran, Y., & Ning, L. (2022). Optimal control and cost-effectiveness analysis for a COVID-19 model with individual protection awareness. *Physica A: Statistical Mechanics and Its Applications, 603*, 127804. https://doi.org/10.1016/j.physa.2022.127804

Yuliana. (2020). Coronavirus disease (COVID-19): A literature review. *Wellness and Healthy Magazine, 2*(1), 187–192. https://wellness.journalpress.id/wellness/article/view/21026